

Adversarial Examples in Constrained Domains

Ryan Sheatsley
Patrick McDaniel
sheatsley@psu.edu
mcdaniel@cse.psu.edu

The Pennsylvania State University

Nicolas Papernot*
papernot@google.com
Google Brain

Michael J. Weisman
Gunjan Verma
michael.j.weisman2.civ@mail.mil
gunjan.verma.civ@mail.mil
United States Army Research
Laboratory

ABSTRACT

Machine learning algorithms have been shown to be vulnerable to adversarial manipulation through systematic modification of inputs (e.g., adversarial examples) in domains such as image recognition. In the default threat model, the adversary exploits the unconstrained nature of images—each feature (pixel) is fully under control of the adversary. However, it is not clear how these attacks translate to *constrained domains* (e.g., network intrusion detection) that limit which and how features can be modified by the adversary. In this paper, we explore whether constrained domains are less vulnerable than unconstrained domains to adversarial example generation algorithms. We create an algorithm for generating *adversarial sketches*: targeted universal perturbation vectors that encode feature saliency within the envelope of domain constraints. To assess how these algorithms perform, we evaluate them in constrained (e.g., network intrusion detection) and unconstrained (e.g., image recognition) domains. The results demonstrate that our approaches generate misclassification rates in constrained domains that were comparable to those of unconstrained domains (greater than 95%). Our investigation shows that the narrow attack surface exposed by constrained domains is still sufficiently large to craft successful adversarial examples—and thus, constraints do not appear to make a domain robust. Indeed, even if a defender constrains an adversary to as little as five random features, generating adversarial examples is still possible.

KEYWORDS

adversarial machine learning, network intrusion detection, constrained domains

1 INTRODUCTION

Machine learning algorithms are rapidly revolutionizing many industries including transportation [35], finance [2, 46], health care [24], education [21, 40], and security [8, 37, 38, 45]. For the past decade, we have seen a revolution in automation as research has focused on increasing the accuracy, problem size, and applicable domains for these automated learners. The results are promising: the latest learning algorithms have shown previously impossible accuracies for problems spanning multiple domains. However, when an adversary is introduced, the machine learning algorithms and the myriad domains they serve often become vulnerable to an adversary.

One of the directions the field of adversarial machine learning explores is the impact of *adversarial examples*: inputs to machine learning models that an attacker has intentionally designed to cause the model to make a mistake, e.g., misclassify [11]. Within the scope of this research, there have been studies that target particular inputs

through a variety of threat models, with algorithms such as the JACOBIAN-SALIENCY MAP APPROACH [33], CARLINI-WAGNER [4], and PROJECTED GRADIENT DESCENT [27], among others. A recent class of attacks, exposing potentially more serious vulnerability, compute *universal adversarial perturbations* [12, 29]. These perturbations can be precomputed and quickly applied at runtime to arbitrary inputs and still achieve adversarial goals (e.g., misclassification of arbitrary inputs to a class chosen by the adversary). The existence of adversarial examples presents a compelling barrier for sensitive domains that use machine learning. Investigations have shown that no domain (thus far) is immune to this phenomenon; the scope of adversarial examples has been expansive, reaching into image processing [4, 12, 28, 33], malware detection [13, 23], text [9, 20], and even speech recognition [5].

A repeated criticism of adversarial machine learning research is that investigations have almost completely focused on unconstrained domains. Implicit to this argument is that such freedom overestimates the capabilities of an adversary in constrained domains where they are often bound by the semantics of features *and* capable of only controlling a subset of features. It stands to reason that such algorithms used to generate adversarial examples would be less effective in constrained domains. In this work, we consider network intrusion detection as our exemplary constrained domain, using existing network intrusion detection datasets: the NSL-KDD [42] and UNSW-NB15 [30]. Here, *constraints* are defined by the following three characteristics: the values within a feature may be fixed (binary vs continuous), the values of different features may be correlated (TCP flags in packets and TCP as the transport protocol), and some features may not be controllable by an adversary (round-trip times).

Furthermore, while there has been research that has focused on constrained *adversaries*[13?], who are bound in their capabilities (e.g., how many total features can be perturbed or which features are manipulable), we differentiate in that we consider constrained *domains*. Specifically, these constraints describe the kinds of inputs that are *permissible* in a domain (For example, network packets that do not obey the TCP/IP protocol would not be permissible). In this work, we consider the union of both adversary and domain constraints, unlike previous work.

In this paper, we test the hypothesis that constrained domains are less vulnerable to the techniques of adversarial machine learning from two perspectives: from the perspective of traditional adversarial algorithms, and from universal adversarial perturbations. This leads to two approaches in our evaluation. Prior to our evaluation, we identify and extract constraints from a dataset. Then, we develop an augmented algorithm, the ADAPTIVE JSMA (AJSMA),

*Work done while the author was at the Pennsylvania State University

to construct adversarial examples that obey domain constraints. Next, we design a second algorithm, the HISTOGRAM SKETCH GENERATION (HSG), the first attack to compute *adversarial sketches*: universal perturbations used to craft adversarial examples en masse that comply with domain constraints. Other algorithms that produce universal perturbations neither have a mechanism to comply with constraints, nor are they immediately suitable for attacking constrained domains (as described in §3). With both algorithms, we measure the success rate of crafting adversarial examples by attacking models directly in both constrained and unconstrained domains, and find that we were comparably successful in both domains (greater than 95%). Furthermore, we use adversarial examples crafted from a model to attack different learning techniques trained on similar, but not identical, data, demonstrating that adversarial examples can *transfer* in constrained domains (reaching up to 93% for the AJSMA and 100% for the HSG). Finally, we show that even if an adversary maintains attack behavior *and* cannot arbitrarily control certain features *and* must obey the TCP/IP protocol, there is still a surprising amount of exploitable attack surface to craft adversarial examples. We make four contributions:

- (1) We introduce formalism to express constraints and design an algorithm that is able to extract them systematically in the domains we consider. Learning constraints codifies the space of permissible adversarial examples.
- (2) We introduce two algorithms. The ADAPTIVE JSMA, which crafts adversarial examples that obey domain constraints. The HISTOGRAM SKETCH GENERATION, which produces adversarial sketches: universal adversarial perturbations that obey domain constraints.
- (3) We perform experiments where we impose an extreme amount of constraints, to the point where an adversary can only control five random features, and show that adversarial examples can still be crafted with a $\sim 50\%$ success rate within our studied constrained domains.
- (4) We demonstrate promising results for both algorithms, reaching greater than 95% misclassification rates across the datasets used in our experiments. This suggests that our studied constrained domains are as vulnerable as their unconstrained counterparts.

2 BACKGROUND

Adversarial machine learning research in unconstrained domains has been broad. Since the initial observations of Biggio et al. and Szegedy et al. in deep neural networks [1, 41] to the robust attacks from Kurakin et al. and Sharif et al. [25, 36], adversarial examples have matured from, “an intriguing property” to a tangible threat.

The first generation of attacks were formed in the context of “white-box” attacks [4, 12, 33]. Under this threat model, adversarial examples are crafted using information (e.g., model parameters) directly from the model under attack. This represents a worst-case scenario, analogous to an insider threat, since such information would not be easily accessible in most practical contexts. Naturally, this motivates the question: Can an adversary successfully attack a model, *without having direct access to its parameters*? Papernot et al. and Tramèr et al. investigated this question by leveraging *transferability*: an adversarial example crafted from one model will

often be an adversarial example for a different model, even if they are using different training data and/or learning techniques [34, 44]. Through this “black-box,” threat model, an adversary trains a *surrogate* model by using inputs to generate output labels from the victim model, called an *oracle*. Afterwards, the surrogate model is used to craft adversarial examples which are then (with high probability) “transferred” to the victim model.

Concurrently, others have investigated what limitations (if any) exist for adversarial examples. Kurakin et al. and Brown et al. explored how adversarial examples can be applied directly to the physical domain, introducing techniques that produce adversarial examples robust to physical distortions, such as rotation, scale, and other transformations [3, 25]. Moreover, Goodfellow et al. and Moosavi-Dezfooli et al. analyzed *universal adversarial perturbations*: single perturbation vectors used to quickly craft adversarial examples from many inputs not known in advance [12, 29]. These universal perturbations are particularly concerning as they enable adversaries to take computation offline and amortize computational costs over many inputs. At present, we are observing an evolution in the way adversarial examples manifest. Each generation contributes to a growing threat against deployed machine learning systems.

For this work, we modify an existing attack, the *Jacobian-based Saliency Map Approach*, introduced by Papernot et al. [33]. The “JSMA” produces an adversarial example by iteratively applying perturbations to the most salient features in an input. The algorithm terminates when either the input is successfully misclassified or the specified l_0 distance¹ is reached. The JSMA greedily selects features to perturb by constructing *saliency maps*, which encode the influence features have over misclassifying a particular input. This l_0 minimization makes the JSMA an attractive candidate for our evaluated domain, as discussed in §3. However, the JSMA is not necessary for crafting adversarial examples in constrained domains. Different attack algorithms can be used, with some adjustments, as reviewed in §3, which we defer to future work. For our study in constrained domains, the JSMA was simply the most readily usable algorithm to leverage.

3 METHODOLOGY

In this section, we explain the intuition behind generating adversarial examples in constrained domains.

3.1 AML in Constrained Domains

Throughout, both in this section for examples and in the evaluation, we will focus principally on network intrusion detection data (specifically, the use of TCP/IP) due to the constrained nature of the domain. Here, we assume a network intrusion detection system classifies feature vectors (representing network traffic flows) as benign or malicious². These feature vectors are created through a feature extraction algorithm, which accepts network packets as input. Therefore, the adversary seeks to bypass the network intrusion detection system by tweaking malicious network traffic (guided by adversarial machine learning techniques), so that it is subsequently classified as benign. Naturally, the adversary must obey the TCP/IP

¹Most attack algorithms have upper limits on the allowable distortion they can introduce. This distortion is defined to be the distance between an adversarial example and its original counterpart. There are many metrics (principally l_p norms [4]) used throughout the literature to measure this distance.

protocol so that the network attacks can be realizable. Any feature vector that violates the TCP/IP protocol (such as negative port numbers) would be manifestly adversarial.

3.2 Challenges in AML with Constraints

Crafting adversarial examples in constrained domains is a necessarily different process from crafting adversarial examples in unconstrained domains. Not all features represent the same kind of information (pixels vs packet information), nor do they describe the same kind of statistical data (discrete vs a blend of categorical, continuous, and discrete). These differences change the threat surface and the underlying assumptions surrounding the capabilities of an adversary in constrained domains. Existing algorithms are unsuitable for attacking constrained domains for these reasons:

(1) *Existing algorithms are largely optimized for human perception.* While there is an open discussion on the amount and kinds of distortion that are appropriate [4], existing algorithms have been tuned for image domains [4, 12, 28]. That is, these algorithms try to minimize human perception of the distortion introduced in adversarial examples. However, such metrics have no meaning for many constrained domains because they are not perceived by humans. Thus, using algorithms optimized for human perception offers us limited utility.

(2) *Existing algorithms assume adversaries have full control over the feature space.* Most algorithms perturb the entire feature space to minimize an l_p norm as a surrogate for estimating a measure of human perception [4, 12, 28]. This is likely an unreasonable assumption in constrained domains. For example, in network intrusion detection, features can represent broad network behaviors that exist outside the control of an adversary, e.g., round-trip times.

(3) *Existing algorithms do not consider domain constraints.* Crafting adversarial examples that obey domain constraints is necessary to mount practical attacks. However, prior works strategically applied perturbations in order to avoid constraints [13, 23] (such as only adding bytes at the end of a binary). While a reasonable strategy for the studied domain (malware), it may not be effective if the adversary can only perturb features that are constrained. As an example of a constraint, network intrusion detection datasets commonly have protocol and service (port number) as features and certain services are exclusive to certain protocols. Therefore, to produce an adversarial example that is representative of a legitimate traffic flow, algorithms need to enforce these constraints.

3.3 Crafting with Constraints

In this subsection, we describe how we learn constraints and incorporate them into crafting adversarial examples.

Learning Constraints. If the constraints are not explicitly given, then they must be inferred. One of the first requirements for properly modeling the constraints of any modeled domain is to codify the specific relationships between features. One of the most important of these relationships is the notion that we introduce as a *primary feature*. Intuitively, a primary feature is a feature that, when

²Without loss of generality, the models we use in the evaluation discriminate between different kinds of network attacks (as well as benign traffic). Nonetheless, the goal of the adversary remains unchanged.

set to particular value, limits the range of permissible values for other features. Conversely, a *secondary feature* does not impose any limitations for other features. Therefore, the first task is to identify primary features and the relationships from these primary features to secondary features. Interestingly, primary features may have relationships amongst themselves, as well as secondary features.

As an example, many popular network intrusion detection datasets include features that represent services, packet flags, and other protocol-related information. Since these features share a causal relation with protocols, we designate transport layer protocols to be primary features and the others as secondary features³. As another example, we could designate using SSL as a primary feature, which would imply using TCP as the transport protocol, which finally dictates the values for other secondary features. Table 5 in the Appendix demonstrates the constraints for one of our evaluated datasets.

Given that constraints are restrictions on where and how features can be perturbed, it is intuitive to model these constraints as a simple form of first-order logic. Here, primary features are the predicates in logical expressions that determine the properties (e.g., values) that a collection of variables (e.g., secondary features) can have. Said alternatively, the set of primary features are the conditionals on the values of other secondary features. Formally, we can understand constraints to have the following form:

$$\forall \mathbf{x} \in \mathbb{X} : \mathbf{x}_k \Rightarrow (\mathbf{x}_1 \in \mathbb{Y}_1) \wedge (\mathbf{x}_2 \in \mathbb{Y}_2) \wedge \dots \wedge (\mathbf{x}_n \in \mathbb{Y}_n)$$

where \mathbf{x} represents an input in a dataset \mathbb{X} , k is a primary feature, and \mathbb{Y}_n represents the values permissible by the semantics of feature n (e.g., $\{0, 1\} \in \mathbb{Y}$ if the feature is binary, or $\{\mathbb{R} : 0 \leq y \leq 1\} \in \mathbb{Y}$ if the feature is continuous). For example, we can represent a simple TCP constraint as follows:

$$\forall \mathbf{x} \in \mathbb{X} : \mathbf{x}_{TCP} \Rightarrow \mathbf{x}_{port} \in [1, \dots, 65535]$$

There are many existing algorithms that can learn constraints from logic [7], as inputs can be modeled as simple instantiations of expressions (i.e., *propositions*). Here, we use primary features to design an algorithm to learn these constraints.

After primary features have been identified, we begin to learn constraints based on the following heuristic: a constraint exists between a primary feature k , and any other feature p , if there exists at least one input in the training set where both k and p are seen together. For example, features that describe TCP packet flags (i.e., p) would have the value 1.0 for TCP traffic flows (i.e., k) and 0.0 for non-TCP traffic flows. Therefore, TCP packet flag features are *constrained* to TCP flows. Conceptually, these constraints encode the maneuvers that are possible (and probable) for an adversary⁴.

Addressing Constraints. To address the challenges discussed prior, we integrate *constraint resolution* into the crafting process. This guarantees that generating an adversarial example obeys not only the semantic constraints of the domain, but also the probabilistic constraints of the dataset as well. As an artifact of our constraint learning process, we may also learn constraints that are technically allowable within the semantics of the domain, but are simply never

³We identified our primary features based on our understanding of the domain and observations in the data. We explore methods to systematically discover primary features when domain expertise is unavailable in §6.

⁴In §5, we also perform experiments where we further add additional constraints that an adversary would have to obey.

observed in the dataset. As a second technique, we also simultaneously minimize the total number of features perturbed (i.e., l_0) to obey constraints and comply with the limited control over features an adversary may have.

Measuring Distance. The distance between an adversarial example and its original counterpart is a measurement of the distortion introduced by an algorithm, commonly represented by an l_p norm. Most algorithms have either limits on the maximum allowable distortion or explicit termination conditions when a particular amount of distortion is introduced. There is debate on the most appropriate distance measure (i.e., the choice of l_p norm) to use for modeling levels of human perception [4]. Our study of constrained domains departs from this debate, as most of these domains are not inherently visual. Therefore, we argue that measuring distance under the l_0 norm is appropriate for our purposes. In particular, we choose l_0 to model how an adversary may be limited to controlling certain features, to enforce domain constraints, and because we are not optimizing for human perception.

Augmenting the JSMA. Before we can use the JSMA in constrained domains, we make a slight adjustment to the algorithm so that it can better search the space of possible adversarial examples. By default, the JSMA parameter θ determines the magnitude and direction of a selected perturbation. A positive θ will increase feature values and a negative θ will decrease them. To allow an adversary more freedom when crafting adversarial examples, we modified the JSMA to perturb in either direction dynamically. This directly improved the success rate of the JSMA. We refer to this modified version as the A(DAPTIVE) JSMA.

To allow the AJSMA to perturb in either direction, we simply evaluate both masks used in [33] that are applied to the saliency map when θ is positive or negative. Formally, for any feature i to be a perturbation candidate, i must satisfy:

$$\left(\frac{\partial f_i(\mathbf{x})}{\partial x_i} > 0 \text{ and } \sum_{j \neq i} \frac{\partial f_j(\mathbf{x})}{\partial x_i} < 0 \right) \text{ or } \left(\frac{\partial f_i(\mathbf{x})}{\partial x_i} < 0 \text{ and } \sum_{j \neq i} \frac{\partial f_j(\mathbf{x})}{\partial x_i} > 0 \right)$$

where $\frac{\partial f_i(\mathbf{x})}{\partial x_i}$ represents the forward derivative for a model f and target class t with respect to feature i in an input \mathbf{x} . Conceptually, the AJSMA only considers features to be perturbable if the target gradient and sum of non-target gradients are in opposing directions. Intuitively, this simply means that any perturbation reduces the distance to the target class or increases the distance to non-target classes.

This modification enables us to determine the optimal perturbation direction for increasing (the left half of the mask) or decreasing (the right half of the mask) features. Afterwards, we use the scoring metric found in [33] and return the most influential feature with the optimal perturbation direction.

Integrating Constraints into the AJSMA. Integrating constraint resolution distills to preventing the AJSMA from selecting features that violate constraints. Once a feature is selected for perturbation, we check if this feature is constrained to a primary feature⁵. This check is described by Algorithm 1.

⁵We note that any additional perturbations made by our constraint resolution algorithm are included when we measure the distance between an original input and an adversarial example. To this effect, adversarial examples that obey domain constraints do not violate l_0 norms.

Algorithm 1: RESOLVING CONSTRAINTS

p is a candidate feature, Γ is the search domain, S is the saliency map for the current input \mathbf{x} , $h : \mathbb{K} \mapsto \mathbb{V}$ is an associative array containing constraints.

```

Input:  $p, \Gamma, S, \mathbf{x}, h$ 
//  $p$  is a primary feature
1 if  $p \in \mathbb{K}$  then
2    $\Gamma = \Gamma \cap h(p)$ 
3    $\mathbf{x}_p \leftarrow$  switch primary feature to  $p$ 
4 end
//  $p$  is constrained to exactly one primary feature
5 else if  $\exists! k \in \mathbb{K}$  s.t.  $p \in h(k)$  then
6    $\Gamma = \Gamma \cap h(k) \setminus \{p\}$ 
7    $\mathbf{x}_k \leftarrow$  switch primary feature to  $k$ 
8 end
//  $p$  is constrained to multiple primary features
9 else if  $\exists k \in \mathbb{K}$  where  $p \in h_k$  then
10   $\Gamma = \Gamma \setminus \{p\}$ 
11   $k' \leftarrow$  the current primary feature in  $\mathbf{x}$ 
    //  $\mathbf{x}$  is using an illegal primary feature wrt  $p$ 
12  if  $p \notin h(k')$  then
13     $k = \arg \max_{\{k \in \mathbb{K} | p \in h(k)\}} S_k$ 
14     $\Gamma = \Gamma \cap h(k)$ 
15     $\mathbf{x}_k \leftarrow$  switch primary feature to  $k$ 
16  end
17 end
//  $p$  constrains all primary features
18 else if  $\forall k \in \mathbb{K}, p \in h_k$  then
19    $\Gamma = \Gamma \setminus \{p\}$ 
20 end
21 if switched primary feature to  $k$  then
    // ensure  $\mathbf{x}$  is not using illegal features
22    $\forall i \notin h(k), \mathbf{x}_i \leftarrow 0$ 
23 end
24 return  $\Gamma, \mathbf{x}$ 

```

Consider the following example using the Algorithm 1. A UDP traffic flow is given to the AJSMA. After analyzing the saliency map, the AJSMA suggests that the current service, TFTP_U , should be switched to FTP , which is a service constrained to TCP. After the service switch is made, the perturbed input is presented to Algorithm 1 to check whether or not any constraint is violated. The first condition determines if the perturbed feature p is a primary feature (i.e., TCP, UDP, or ICMP). In this example, it is not, so we move to the second condition and evaluate if p is constrained to exclusively one primary feature. In this case, p is exclusively associated with TCP. Thus, the search domain is further restricted to TCP-compliant features and the transport protocol of the input is switched from UDP to TCP. Since the input has switched primary features from UDP to TCP, we finally set all non-TCP features to 0. Once the AJSMA terminates, the produced adversarial example will be representative of a permissible traffic flow, i.e., it obeys the domain constraints.

3.4 Creating Adversarial Sketches

In this subsection, we describe how we create adversarial sketches⁶: universal perturbations that obey constraints.

⁶The concept of “sketching,” also known as *approximate query processing* [6], was first introduced by Flajolet et al. Sketching refers to a class of streaming algorithms that seek to extract information from a data stream in a single pass [10]. Commonly deployed in memory-constrained environments, these algorithms approximate or summarize the information in a given data stream. Adversarial sketches are similar as they are an approximation of a universal perturbation and computed through one pass of inputs.

For the same reasons described at the beginning of §3, existing algorithms to generate universal adversarial perturbations [3, 15, 29] are not immediately usable in constrained domains: the algorithms are largely optimized for human perception, they assume adversaries have full control over the feature space, and they do not consider domain constraints.

In our search for adversarial sketches in constrained domains, we take a principled approach using two tools: adversarial examples generated from the AJSMA and a *perturbation histogram*. Prior to the algorithms mentioned earlier for computing universal adversarial perturbations, encountering these perturbations was a matter of chance: an adversary would be required to apply a perturbation generated from an attack on other unperturbed inputs and simply observe the universality of the perturbation, i.e., brute-forcing the universal perturbation [12].

Adversarial Examples from the AJSMA. Initially, we followed the same brute-force approach in [12]: we used adversarial examples crafted from the AJSMA to glean insights for universal perturbations. This brute-force approach is feasible (in terms of computational complexity) for network intrusion detection datasets as their dimensionality and cardinality is small. After evaluating every perturbation generated by the AJSMA on every input in the test set, we discovered a handful of universal perturbations.

Perturbation Histograms. The perturbation histogram encodes how perturbations are distributed en masse (an example is shown later in §4). To produce the histogram, we enumerate over all of the perturbations generated by the AJSMA (including any additional perturbations made to resolve constraints) and record the perturbed features and directions. Our insight for the histogram is rooted in how the AJSMA scoring metric ranks influential features; we hypothesized that features commonly perturbed across inputs from different classes would be optimal candidates for building an adversarial sketch. This hypothesis was reinforced by our observation that the perturbation histogram was (relatively) static: random shuffling of partitioned training sets, unique training parameters, and random subsets of analyzed adversarial examples yielded minor changes to the perturbation histogram. These substantial adjustments to our experiment workflow demonstrated little change between perturbation histograms. These observations suggest that the perturbation histogram is a combined representation of class-based saliency *and* domain constraints.

With the universal perturbations discovered through the AJSMA and the static nature of the perturbation histogram, we made an observation: **the majority of the perturbed features (and their associated directions) in the most successful universal perturbations generated from the AJSMA mapped directly to the most perturbed features in the perturbation histogram. This key observation led us to the creation of the *Histogram Sketch Generation*.**

Histogram Sketch Generation. The HISTOGRAM SKETCH GENERATION accepts a perturbation histogram H and integer n as parameters and returns an adversarial sketch a , which consists of the top n most frequently perturbed features and optimal directions⁷. We observed that the most successful universal perturbations generated by the AJSMA had a subset of features that directly mapped to the most frequently perturbed features in the perturbation histogram.

Intuitively, if we consider these successful universal perturbations as the optimal solution, then the HSG approximates the optimal solution by returning a subset of those features (and associated directions). Figure 6 in the Appendix demonstrates a handful of sketches.

It is interesting to note that the HSG is essentially the problem of variable selection in classical statistics. Variable selection involves the selection of a subset of relevant variables (or features) in the model, such that a “minimal” amount of information is lost (e.g., minimal impact on model loss). Many common procedures in classical statistics, such as LASSO or stepwise regression, aim to balance model fit with a penalty on the l_0 norm (or a relaxation of this norm to l_1 , in the case of LASSO)[43]. Our approach of greedily selecting the top n most perturbed features is directly analogous to stepwise regression’s (greedy) selection of the n features which best explain the data. As the complexity grows combinatorially with the number of features, greedy methods are necessarily resorted to, and our approach here is no exception.

4 EVALUATION

In this section, we evaluate our approach on two network intrusion datasets, the NSL-KDD and the UNSW-NB15, as well as two image recognition datasets, the GTSRB and MNIST. In our evaluation, we answer two questions:

- (1) Are constrained domains more robust against adversarial examples?
- (2) Do universal adversarial perturbations exist in constrained domains?

Our experiments revealed that: we can craft adversarial examples with success rates greater than 95%, even in the presence of constraints; we can compute highly successful adversarial sketches, reaching greater than 80% misclassification rates for the majority of learning techniques.

Our experiments were performed on a Dell Precision T7600 with an Intel Xeon E5-2630 and a NVIDIA GeForce TITAN X. We used Cleverhans 2.0.0 [32] for training our models and crafting adversarial examples.

4.1 Datasets

Before we describe our experiments, we provide an overview of the four evaluated datasets and any preprocessing that we performed. Table 1 describes the model architectures, hyperparameters, and model accuracies across all four datasets⁸.

We evaluate our approach on two network intrusion detection datasets for the application of constrained domains and two image classification datasets for unconstrained domains. We use these two image classification datasets for comparison with other works

⁷While the HSG does not take a target class as a parameter, it uses information directly from the perturbation histogram to create an adversarial sketch. As a consequence, the HSG will return a targeted adversarial sketch if the histogram is built from targeted adversarial examples.

⁸Note that while the accuracy of our network intrusion detection models sit around 77%, these are consistent with the literature [17, 19, 42?]. Notably, Tavallae et al., who initially uncovered the inherent problems with the KDD CUP 99 (which resulted in the creation of the NSL-KDD), reported 77.41% accuracy with Multi-layer Perceptrons [42]. Furthermore, Moustafa et al., who designed the UNSW-NB15 to address the shortcomings of the NSL-KDD [30], reported 81.34% accuracy (using the full training set) with an artificial neural network [31]. These accuracies are comparable to the highest to date.

in adversarial machine learning as well as a demonstration of the cross-domain applicability of our approach. Note that these are unconstrained domains (i.e., images), and thus the AJSMA behaves similarly to the original JSMA (other than that it can perturb in either direction).

Dataset	Architecture	Units	Batch Size	Learning Rate	Epochs	Testing Acc.
NSL-KDD	MLP	123, 64, 32, 5	200	0.01	5	77% \pm 1.0%
UNSW-NB15	MLP	196, 98, 49, 10	128	0.01	10	75% \pm 1.2%
MNIST	CNN	784, 128, 128, 10	128	0.001	6	98% \pm 0.1%
GTSRB	CNN	2700, 128, 128, 42	128	0.001	6	82% \pm 2.0%

Table 1: Model Information

NSL-KDD. The NSL-KDD dataset is an improved variant of the KDD Cup99 dataset [42]. The KDD Cup99 (and its NSL-KDD successor) have been used widely in the network intrusion detection community. We chose to use the NSL-KDD for the novel application of adversarial examples in this field, familiarity of the dataset within the academic community, and the lack of well-formed network intrusion detection data.

The NSL-KDD contains 5 classes, with 4 attack classes and 1 benign class. It contains 125,973 samples for training and 22,543 samples for testing. It contains 41 features⁹, separated into four high-level categories of features: basic features of TCP connections, content features within a connection suggested by domain knowledge, traffic features that are computed using a two-second time window, and host-based features. The NSL-KDD has been widely studied and so we defer to prior work [8, 42] for the subtle details of the dataset.

UNSW-NB15. The UNSW-NB15 dataset was designed to be an updated version of the NSL-KDD, containing modern attacks that express a “low footprint” [30]. The Australian Centre for Cyber Security (ACCS) used the *IXIA PerfectStorm* tool to create a combination of normal and abnormal network traffic. The abnormal traffic generated from the *IXIA PerfectStorm* tool is broken down into nine attack types, which we used as our source classes for generating our adversarial examples¹⁰. After the traffic is generated, the authors leveraged *Argus* and *Bro-IDS* tools to construct reliable features.

The UNSW-NB15 contains 10 classes, with 9 attack classes and 1 benign class. It contains 175,341 samples for training and 83,332 samples for testing. The dataset contains 48 features, separated into four high-level categories of features: flow-based, basic connection, content, and time-based. We defer to the authors for a comprehensive description of the dataset [30] and its similarity with the NSL-KDD [31?].

MNIST. The Modified National Institute of Standards and Technology database contains handwritten digits. We chose to use MNIST due to its simplicity, to demonstrate cross-domain applicability of our approach, and to have a direct comparison with other adversarial machine learning approaches.

⁹We used the post-processing options in WEKA [14], an open-source data mining framework, to convert categorical features to one-hot vectors.

¹⁰While the authors intended this dataset to be used for benchmarking anomaly detection algorithms, we used it as a *signature-based* dataset by using the last feature, “attack class,” as the label. We achieved high classification accuracies, and thus argue that our modification has no impact on the significance of our results found in the evaluation of our methodology.

The MNIST database contains 10 classes, with numerical digits from 0 through 9. It contains 60,000 samples for training and 10,000 samples for testing. Unlike the network intrusion detection datasets, no preprocessing was required to integrate this dataset into our experimental setup. We were able to use the dataset directly as-is. We defer to the authors for the intricate details surrounding the MNIST dataset [26].

GTSRB. The German Traffic Sign Recognition Benchmark is a dataset of common traffic signs found throughout Germany. We chose to use the GTSRB to for its increased complexity over MNIST and as a second example of the cross-domain applicability of our methodology.

The GTSRB contains 42 classes. After preprocessing, our experiments contained 21,792 samples for training and 6,893 samples for testing. Throughout the dataset, there are identical images of varying sizes. We first cropped the region of interest (which contains the traffic sign) and downsampled to a final size of 30×30 . For more details concerning the GTSRB, we defer to the authors [39].

4.2 Experiment Overview

In this subsection, we describe our experiments in detail, using the NSL-KDD as an application of our approach.

Through our evaluation on network intrusion detection, we note that our experiments emulate a realistic adversary by taking different attacks and masking them as benign traffic.

Data Curation. We perform a stratified shuffle-split on the training set into five parts. Splitting our training set into five parts lays the foundation for measuring transferability: each partition (which we refer to as A, B, C, D, E) is representative of a uniquely trained model (which we refer to as M_A, M_B, M_C, M_D, M_E respectively), mirroring the setup described in [34]. This setup allows us to measure *intra-technique* transferability rates: the rate at which adversarial examples crafted from one model are also misclassified by another model with the same learning technique. Furthermore, we can also measure the converse, *inter-technique* transferability: the same misclassification rate except with a model of an entirely different learning technique¹¹. Note, that *transferability* is not the same as a black-box attack; we do not use the output of an oracle to label data for a surrogate model, as shown in [18, 34]. While transferability *enables* black-box attacks, they are not the same, as transferability has been observed prior to the inception of black-box attacks [12, 41].

Next, we perform a stratified shuffle-split on the test set. This creates two sets of isolated inputs: we use the AJSMA on one set and the HSG on the other. This is to ensure that the sketches are only applied on inputs that had no influence in the creation of the sketch (recall that we analyze the adversarial examples created by the AJSMA to build sketches). Furthermore, the stratified shuffle-split of the test set is to ensure that the AJSMA crafts adversarial examples from inputs spanning all classes. This enables us to create

¹¹For our inter-technique evaluation, we consider four popular learning techniques: Logistic Regression (LR), Decision Trees (DT), Support Vector Machine (SVM), and K-Nearest Neighbors (KNN). Each one of these learners represent different learning paradigms (and are popular in commercial and academic contexts), and are thus appropriate candidates for evaluating inter-technique transferability. Hyperparameters and other details can be found in the Appendix.

Protocol	Feature Type				Total
	Basic	Content	Timing-based	Host-based	
TCP	81	12	9	10	112
UDP	12	0	7	8	27
ICMP	14	0	7	8	29

Table 2: NSL-KDD constraint distribution, categorized by feature type - Unlike TCP, UDP and ICMP have limited degrees of freedom.

effective adversarial sketches, as all class-specific information is distilled into the perturbation histogram.

Using the NSL-KDD as an example for the first stage, we built a Multi-layer Perceptron with 4 layers: an input layer of 123 units, fully-connected to 64 units, fully-connected to 32 units, and finally an output layer with 5 units¹². The output layer conveys our 5 classes: Normal (Benign), Probe, Denial of Service (DoS), User to Root (U2R), and Remote to Local (R2L). We used rectified linear units (ReLU) as our chosen activation function for our hidden layers and softmax at the output layer. Our models are trained via the Adam optimizer [22] with a batch size of 200 and a learning rate of 0.01 for 5 epochs. With our five splits, each model, M_A through M_E , is trained with $\sim 25,194$ inputs. With these hyperparameters, network architecture, and training set size, we were able to achieve an average $77\% \pm 1.0\%$ accuracy on the test set, which is consistent with the literature [17, 19, 42?].

Constraint Generation. With the heuristic described in §3, we learn constraints in the NSL-KDD with PROTOCOL as the primary feature. The intuition behind this selection is straightforward: a majority of the features in the NSL-KDD describe metadata surrounding these protocols, e.g., flag information, services, and content-related features like FTP commands. The distribution of the extracted constraints for the NSL-KDD can be found in Table 2. We observe that the TCP protocol offers the highest degree of maneuverability by a wide margin (and to no surprise as it constitutes the majority of traffic flows in the dataset). This is unlike UDP and ICMP, who are significantly more constrained. Table 5 in the Appendix shows all of the constraints, sorted by feature type.

Adversarial Example Generation. To investigate the first question in our evaluation, we craft adversarial examples with the AJSMA. With the constraints integrated into the crafting process, we iterate over the first half of the test set for each model, M_A through M_E , and craft adversarial examples (the second half of the test set is used to craft adversarial examples via the sketches produced by the HSG). Table 3 describes the output of this stage from an example NSL-KDD run with “Benign” (0) as the target class. Figure 1 demonstrates the perturbation histogram computed from the same run.

We note that there are particular features that were consistently perturbed in nearly all adversarial examples, namely setting the service as IRC and increasing NUM_ACCESS_FILES¹³. To understand

¹²We note that the number of layers and units was influenced by research that suggests an optimal upper bound for the number hidden neurons for feed-forward networks [16]. The remainder of our hyperparameter selection follows no formal process.

AJSMA Experiment Results - Target 0 “Benign”	
Testing Inputs	11,272
Labeled as Target Class	4,856
Misclassified as Target Class	2,532
Number of Inputs Attacked	3,884
Average Distortion	3.39% \sim 4.18 features
Class Success Rates	0:NaN, 1:100%, 2:99% 3.99%, 4:100%

Table 3: Output from crafting adversarial examples with the AJSMA for NSL-KDD model, M_B - Even domains with constraints are vulnerable to adversarial examples.

why, we used WEKA [14] to analyze the distribution of these features, which revealed a trivial explanation: inputs that use IRC as the service and have high values for NUM_ACCESS_FILES are heavily skewed towards our target class, “Benign”. Figure 2 shows these distributions (Note that the “Benign” target class is bottom class (0) on the Y-axis).

Adversarial Sketch Generation. To investigate the second question in our evaluation, we use the perturbation histogram (computed from adversarial examples crafted by the AJSMA) to create adversarial sketches. As described in §3, the HSG creates adversarial sketches by selecting the top n most perturbed features from the perturbation histogram. Finally, we craft adversarial examples by applying the sketch to the second half of the test set, for each model, M_A through M_E .

4.3 Measuring Success

With the adversarial examples crafted via the AJSMA and HSG, we measure the effectiveness of the two algorithms through white-box attacks and through transferability. We define the success rate of white-box attacks as the number of adversarial examples misclassified as the target class over the total number of attempted inputs, formally:

$$SR_{wb} = \frac{|\{\mathbf{x} \in \mathbb{X} : f(\mathbf{x}) = t\}|}{|\mathbb{X}|}$$

where \mathbb{X} represents the set of attempted inputs, f is a model, and t is the target class. Furthermore, we define the transferability success rate to be the number of adversarial examples misclassified as the target class by the target model over the number of successful adversarial examples crafted from the source model, formally:

$$SR_{transfer} = \frac{|\{\mathbf{x} \in \mathbb{X} : f'(\mathbf{x}) = t\}|}{|\{\mathbf{x} \in \mathbb{X} : f(\mathbf{x}) = t\}|}$$

where \mathbb{X} again represents the set of attempted inputs from the source model f , and f' represents the target model.

AJSMA Results. In Table 4 (a) on the left, we show the NSL-KDD AJSMA success rates for white-box attacks and transferability rates. The labels on the left represent the source model used to generate

¹³While it may seem this feature is not derived from network data, both the NSL-KDD and UNSW-NB15 have a “high-level content” category of features, which are derived from payload information.

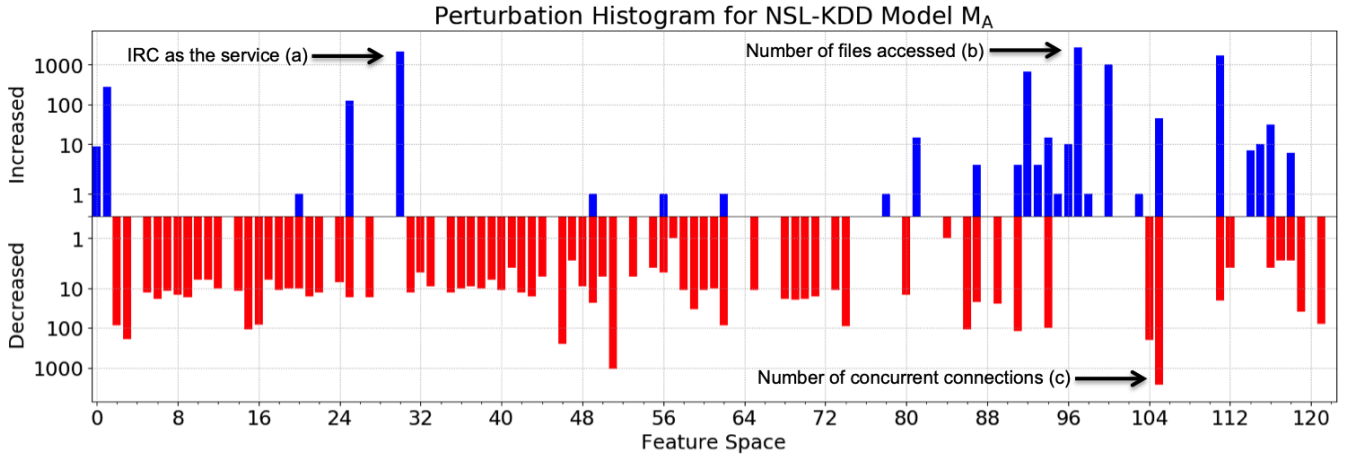


Figure 1: NSL-KDD model M_B Perturbation Histogram produced by adversarial examples from the AJSMA in log scale - Certain features are *consistently* increased (a) & (b) and decreased (c), indifferent of the source class.

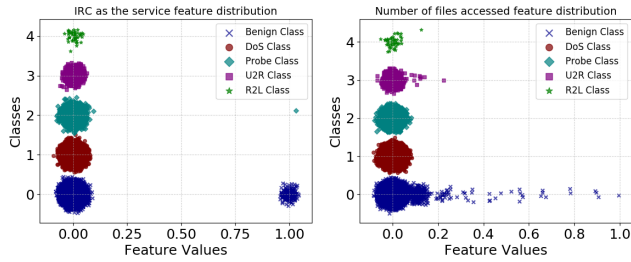


Figure 2: NSL-KDD class distribution for `SERVICE=IRC` (a) and `NUM_ACCESS_FILES` (b) - These two features are often perturbed due to their bias towards the “Benign” class, shown as class 0 on the Y-axis.

adversarial examples and the labels on top represent the target models that were attacked. For the intra-technique case, the white-box results can be read along the diagonal (as the source and target are the same model). For both intra- and inter-technique cases, the transferability rates are represented in all other cells. The AJSMA was broadly successful in creating targeted adversarial examples while introducing relative amounts of distortion comparable to image-based experiments, even in the presence of constraints. These results suggest that the constraints for our evaluated domain do not offer any robustness against adversarial examples.

Additionally, it is interesting that the adversarial examples produced by the AJSMA had notable transferability rates in intra-technique case (an average of 73% across our network intrusion detection experiments). This would suggest that transferability is stronger in lower dimensional spaces.

HSG Results. In Figure 3, we show NSL-KDD model M_B success rates for intra- and inter-technique transferability for varying values of n between 1 and 11. There are broad regions for values of n which have high success rates, reaching 100% in white-box settings and greater than 80% transferability rates for the majority

of learning techniques. Indeed, it would appear that the most often perturbed features (by the AJSMA) are appropriate candidates for building an adversarial sketch. Furthermore, these results confirm the existence of universal adversarial perturbations that obey domain constraints.

Finally, we are surprised at the fragility of the models trained on network intrusion detection data; sometimes perturbing only *three* features was needed to misclassify greater than 80% of inputs in the test set. We believe that this fragility is partly a function of the skewed distribution certain features can have for specific classes, such as the ones shown in Figure 2. This insight is unlike the adversarial examples crafted in image domains, where high dimensionality and a more balanced class distribution for features appear to mitigate this fragility.

Table 4 shows the success rates for both of our algorithms across all four datasets. The values of n listed equal $\sim 4\%$ l_0 distortion for the HSG. Again, the labels on the left represent the source model used to generate adversarial examples, while the labels on top represent the target models that were attacked. For the intra-technique case, the white-box results can be read along the diagonal (as the source and target models are the same). The transferability rates, for both intra- and inter-technique cases, are represented in all other cells.

We observe high success rates for both the AJSMA and the HSG in both white-box attacks and transferability for several of the datasets. While the AJSMA struggled significantly to produce adversarial examples that transferred as the dimensionality increased, the HSG transferability rates were more resilient (but still affected)

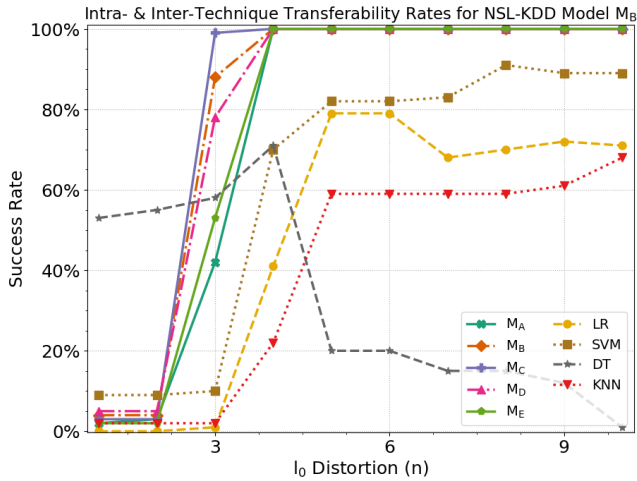


Figure 3: HSG intra- and inter- transferability rates for NSL-KDD model M_B for target “Benign” as a function of l_0 distortion n - Values between 6-9 for n have greater than 70% misclassification for most learning techniques.

to the increased dimensionality¹⁴. This would suggest that the distance between decision boundaries increases as model complexity increases, thus mitigating transferability for our algorithms.

From our investigation, we highlight some key takeaways:

- (1) Constraints, as they stand, are not problematic for crafting adversarial examples in the domains we studied. The AJSMA reached 100% success rates for most attempted inputs, with distortion rates comparable to image-based experiments, while in the presence of constraints.
- (2) Universal adversarial perturbations that obey domain constraints exist. The HSG produced Adversarial Sketches that reached 100% success rates in constrained domains for a values of n that represent $\sim 4\%$ l_0 distortion. Furthermore, they produced adversarial examples that had higher transferability rates than the AJSMA.
- (3) Network intrusion detection data is highly fragile: a small dimensionality and biased distributions enable attack algorithms to alter very few features to successfully craft targeted adversarial examples.
- (4) Worst-case scenarios (i.e., white-box attacks) are highly vulnerable, not surprisingly. With direct access to model parameters, an adversary can have a sophisticated level of control over the output of a model.
- (5) Network intrusion detection data appears to be highly vulnerable to transferability attacks. Even in the presence of disjoint training sets and different learning techniques, both

¹⁴We hypothesize that this is partly due to how the AJSMA is designed. Conceptually, the AJSMA creates adversarial examples that *just* cross over the decision boundaries. While the decision boundaries among models of lower dimensionality may be similar (and thus, an adversarial example can cross over the decision boundaries of multiple models), this appears to be untrue for models of higher dimensionality, where there can be multiple unique ways to separate the data. We could test this by regularizing high dimensional models. Furthermore, we could also alter the design of the AJSMA to continue adding additional perturbations so that it returns an adversarial example that is more confidently misclassified.

attacks produced adversarial examples with surprising levels (an average of 73% for the AJSMA and 97% for the HSG, for models of the same learning technique) of transferability.

5 UNCONTROLLABLE FEATURES

Throughout this paper, we have discussed some of the differences between adversarial machine learning in constrained domains versus unconstrained domains. One of the most fundamental questions within this community is: *what precisely is an “adversarial example?”* There are varying definitions with different objectives used throughout AML research. In the image space, it has been generally agreed that if an attack algorithm produces perturbations that are undetectable by a human observer, then it is an adversarial example. However, it is not clear how to translate this objective in other domains.

Research outside of image space (usually) provides their own definitions: perturbed malware must maintain its properties of malware [13, 23], perturbed audio must be nearly inaudible [5], perturbed text must preserve its semantics [9, 20], among other definitions. For our work in network intrusion detection, we follow an intuitive definition: perturbed network flows must maintain their attack behavior. For example, a DoS attack must still be a DoS attack post-perturbation.

However, validating attack behaviors is a nontrivial task as security is contextual: a DoS attack on a government network has different behaviors than an attack on a family business. Therefore, any sort of simulation to observe attack behavior must be in a similar context to the one in which the dataset was built from. This is particularly challenging for old datasets like the NSL-KDD, as even a similar network setup would have different behavior given the modern hardware and software on the systems that would constitute that network. Even if all these factors could be accounted for, there are certain classes of attacks whose “success” is challenging to measure. For example, in reconnaissance attacks it is difficult to know if the information gathered by an adversary is useful.

Regardless, all of these points of contention are driven by a single hypothesis: *Perhaps adversarial examples cannot be crafted if features which represent the semantics of the attack cannot be perturbed.* Instead of attempting to justify why any set of features is critical to the semantics of the attack, we take a different stance on addressing this hypothesis: even if some reasonably sized subset of features could not be perturbed (as to not invalidate the attack), we argue that adversarial examples can still be successfully crafted. With the lessons learned through this research, we set out to investigate this hypothesis with a simple experiment.

To test this hypothesis, we iterate over multiple sets of randomly selected features and make them unperturbable by the adversary. We repeat this random selection for sets of varying cardinalities from 1 to 41 features (where 41 represents the entire feature space). We train a new model on the full NSL-KDD training set and use the 100 most representative¹⁵ inputs from each class¹⁶ from the test set. Next, we iterate over all of the possible combinations of

¹⁵We find the most representative inputs by maximizing the difference (via the softmax layer) between the output component that corresponds to the label and the sum of the components that represent all non-label classes.

¹⁶The “R2L” class only had 17 inputs that were correctly classified. Thus, we crafted from 317 inputs as opposed to 400.

ADAPTIVE JSMA										HISTOGRAM SKETCH GENERATION									
	M_A	M_B	M_C	M_D	M_E	LR	SVM	DT	KNN	n	M_A	M_B	M_C	M_D	M_E	LR	SVM	DT	KNN
M_A	100%	69%	51%	51%	61%	34%	40%	34%	20%	6	100%	100%	100%	100%	100%	80%	85%	16%	19%
M_B	73%	99%	72%	78%	67%	49%	50%	39%	44%	M_A	100%	100%	100%	100%	100%	79%	82%	20%	59%
M_C	63%	69%	100%	66%	69%	30%	34%	27%	24%	M_B	100%	100%	100%	100%	100%	65%	83%	50%	34%
M_D	54%	93%	70%	99%	64%	24%	38%	25%	22%	M_C	100%	100%	100%	100%	100%	81%	87%	22%	59%
M_E	83%	79%	71%	66%	100%	42%	55%	41%	17%	M_D	100%	100%	100%	100%	100%	98%	93%	27%	19%
										M_E	100%	100%	100%	100%	100%				
(a) NSL-KDD										(b) UNSW-NB15									
	M_A	M_B	M_C	M_D	M_E	LR	SVM	DT	KNN	n	M_A	M_B	M_C	M_D	M_E	LR	SVM	DT	KNN
M_A	100%	97%	92%	96%	96%	72%	81%	29%	53%	9	88%	99%	95%	96%	96%	99%	96%	29%	37%
M_B	50%	100%	72%	94%	71%	62%	62%	12%	26%	M_B	99%	100%	99%	100%	99%	99%	100%	20%	62%
M_C	73%	81%	100%	93%	87%	71%	76%	19%	49%	M_C	93%	97%	100%	77%	95%	73%	100%	27%	41%
M_D	69%	64%	55%	100%	59%	53%	48%	8%	25%	M_D	80%	99%	100%	100%	99%	74%	99%	13%	30%
M_E	66%	80%	90%	96%	100%	66%	69%	15%	38%	M_E	98%	100%	100%	94%	92%	85%	100%	28%	39%
(c) MNIST										(d) GTSRB									
	M_A	M_B	M_C	M_D	M_E	LR	SVM	DT	KNN	n	M_A	M_B	M_C	M_D	M_E	LR	SVM	DT	KNN
M_A	100%	39%	30%	19%	11%	21%	24%	18%	5%	41	24%	35%	18%	14%	9%	45%	48%	14%	7%
M_B	6%	100%	14%	6%	2%	19%	18%	14%	2%	M_B	17%	42%	14%	15%	54%	62%	61%	13%	5%
M_C	12%	32%	99%	9%	8%	23%	22%	15%	1%	M_C	22%	31%	41%	9%	14%	60%	55%	32%	5%
M_D	17%	44%	26%	100%	21%	21%	21%	19%	5%	M_D	13%	30%	14%	36%	13%	46%	46%	33%	6%
M_E	20%	53%	33%	20%	99%	24%	27%	18%	6%	M_E	15%	29%	11%	12%	31%	44%	58%	21%	4%
	M_A	M_B	M_C	M_D	M_E	LR	SVM	DT	KNN	n	M_A	M_B	M_C	M_D	M_E	LR	SVM	DT	KNN
M_A	97%	2%	1%	3%	2%	0.2%	1%	3%	0%	104	34%	6%	27%	6%	7%	0.2%	2%	12%	0%
M_B	1%	95%	0.5%	1%	1%	0.3%	2%	2%	0%	M_B	9%	27%	14%	2%	8%	0.5%	1%	6%	0%
M_C	2%	2%	98%	2%	0.8%	0.1%	2%	1%	0%	M_C	17%	4%	44%	2%	7%	0.6%	1%	5%	0%
M_D	0.5%	1%	3%	99%	1%	0.2%	0.8%	3%	0%	M_D	29%	12%	16%	29%	12%	1%	1%	5%	0%
M_E	0.7%	2%	1%	2%	94%	0.1%	0.5%	2%	0%	M_E	14%	8%	15%	3%	35%	0.1%	1%	4%	0%

Table 4: Results for AJSMSA (left) and HSG (right) for all of our experiments for target class “Benign” - Values of n for our sketches represent $\sim 4\%$ l_0 distortion.

features made unperturbable to an adversary, i.e., $\binom{41}{k}^{17}$ for $k \in \{1, 2, \dots, 41\}^{18}$. Once we have identified a set of unperturbable features, we simply eliminate that set from initial search domain of the AJSMSA. In this experiment, we crafted a total of 17,664,191 adversarial examples. Figure 4 demonstrates the success rate of the AJSMSA as a function of the number of controllable (i.e., perturbable) features.

The results support our argument: the success rate of AJSMSA begins to decline when the adversary can only control ~ 12 features. Even when an adversary has control over only *five random* features (which represents around $\sim 10\%$ of the feature space), the success rate of crafting adversarial examples (with the most representative forms of an attack) is slightly less than 50%. Furthermore, this result demonstrates that applying more restrictive constraints would have little impact on the success of the adversary.

Finally, we would also like to highlight how this experiment demonstrates a type of constraint not covered in the evaluation section: features that the adversary simply does not have control over. Throughout this work, our constraints were defined via the

¹⁷The NSL-KDD has 41 features before expanding categorical features to one-hot vectors. If a particular combination contains a categorical feature, we eliminate all possible values associated with the feature from the search domain.

¹⁸To prevent combinatoric explosion, we randomly sampled 1,500 unique combinations if the total number of possible combinations for a particular value of k exceeded 1,500. In total, we evaluated 55,723 unique combinations of unperturbable features.

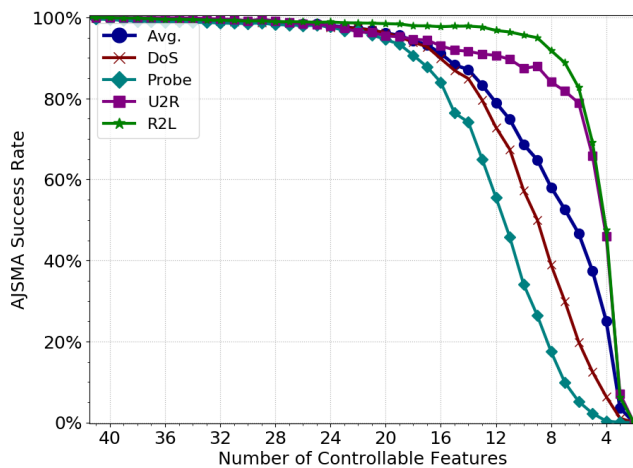


Figure 4: AJSMSA Success Rate with unperturbable features - The overall success rate starts to decrease significantly when the adversary is restricted to controlling ~ 12 features.

semantics of the domain, i.e. the TCP/IP protocol. However, this experiment to preserve the semantics of the attack also serves as

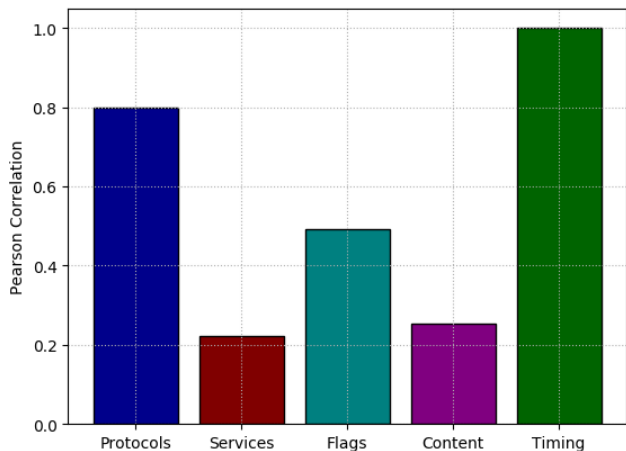


Figure 5: Normalized mean of summed absolute values of Pearson Correlation Coefficients for five categories of features in the NSL-KDD - Protocols are correlated with the majority of features, closely behind timing-based features, which are highly correlated amongst themselves.

a demonstration of the efficacy of an adversary under this second type of constraints. These results suggest that even if an adversary maintains attack behavior *and* cannot arbitrarily control certain features *and* must obey the TCP/IP protocol, there is still a surprising amount of exploitable attack surface to craft legal adversarial examples.

6 DISCUSSION

In this section, we describe our thoughts for future work.

Identifying Primary Features. In this work, we identified primary features manually through not only our understanding of the domain, but observations of the data. We noticed that many features were correlated with the transport layer protocol (as we expected, based on the descriptions of the features). However, we may not always be able to use the descriptions of features to guide us towards identifying primary features. Thus, we hypothesize that primary features could be identified by ranking the features that are most correlated with others. The intuition here is that while secondary features will be highly correlated with primary features, primary features will be highly correlated with the majority of secondary features. We performed a simple experiment where we computed Pearson product-moment correlation coefficients for all features in the NSL-KDD training set. We took the mean of sum of the absolute value of the coefficients for four categories of features as their scores and found protocols to indeed be correlated with the majority of features, as shown in Figure 5. At first, it appeared that timing-based features had a higher correlation than protocols among all features. However, we noticed that the timing-based features were highly correlated *amongst themselves*, which was the largest contributor to their scores (and to no surprise, since many timing-based features are derivatives or direct inverses of one another, e.g., `SAME_SRV_RATE` and `DIFF_SRV_RATE`). Thus, if we eliminate such

functionally inverse and derivative features, this approach would suggest that primary features could be identified systematically.

Defenses. We also hypothesize that constraints *can* be useful in defending against adversarial examples, even though the constraints found in the studied datasets were ineffective. We are interested if constraints in other domains, such as malware and spam, can prove to be effective against adversarial example generation algorithms. It is intuitive that maintaining the behavior of malware while simultaneously perturbing binary code would be a challenging problem.

In addition, we also observe that our approach for building adversarial sketches can also be used by a defender to assess model vulnerability. In particular, a defender could design a simple mechanism (driven by the perturbation histograms) that reveals universal directions that would make the model vulnerable. The defender can then use this analysis to detect adversarial examples at deployment. However, an adversary could circumvent detection by selectively perturbing features that have less impact. Naturally, this would come at a cost of introducing additional distortion and control over more features, which may be impractical for an adversary.

Finally, we note that defenses against adversarial examples, including detection techniques, robust optimization, etc., is an open problem. At present, it is unclear whether or not a generalizable defense exists against adversarial examples.

7 CONCLUSIONS

This paper investigated the impact of adversarial examples in constrained domains through the perspective of traditional adversarial algorithms and universal adversarial perturbations. In addition to this investigation in unique domains like network intrusion detection, we introduced two new algorithms: the `ADAPTIVE JSMA`, which produces adversarial examples in constrained domains, and the `HISTOGRAM SKETCH GENERATION`, which generates adversarial sketches: universal adversarial perturbations that obey domain constraints. Our work demonstrates how adversaries can craft permissible adversarial examples in constrained domains.

Through our experiments, we observed how biased distributions coupled with low dimensionality can have a significant impact on model vulnerability, even in the presence of constraints. Furthermore, we demonstrated how when defender constrains an adversary to *five random* features, adversarial examples can still be crafted with a $\sim 50\%$ success rate.

Prior to our work, the impact of adversarial learning has been largely understood in the context of unconstrained domains. We initially hypothesized that systems whose domains were constrained would be more resilient to attack algorithms. However, our investigation suggests the inverse. Our two algorithms were able to craft adversarial examples with minimal distortion and with success rates of greater than 95% that also transferred to other models at rates up to 93%.

Indeed, it is unclear if any domain is immune to adversarial machine learning. Through a simple number of transformations, an adversary can wholly control a model, thereby defeating systems deployed in sensitive domains.

REFERENCES

- [1] BIGGIO, B., CORONA, I., MAIORCA, D., NELSON, B., ŠRNDIĆ, N., LASKOV, P., GIACINTO,

- G., AND ROLI, F. Evasion attacks against machine learning at test time. In *Joint European conference on machine learning and knowledge discovery in databases* (2013), Springer, pp. 387–402.
- [2] BOSE, I., AND MAHAPATRA, R. K. Business data mining—a machine learning perspective. *Information & management* 39, 3 (2001), 211–225.
- [3] BROWN, T. B., MANÉ, D., ROY, A., ABADI, M., AND GILMER, J. Adversarial patch. *CoRR abs/1712.09665* (2017).
- [4] CARLINI, N., AND WAGNER, D. Towards evaluating the robustness of neural networks. In *Security and Privacy (SP), 2017 IEEE Symposium on* (2017), IEEE, pp. 39–57.
- [5] CARLINI, N., AND WAGNER, D. A. Audio adversarial examples: Targeted attacks on speech-to-text. *CoRR abs/1801.01944* (2018).
- [6] CORMODE, G. Sketch techniques for approximate query processing. In *Synopses for Approximate Query Processing: Samples, Histograms, Wavelets and Sketches, Foundations and Trends in Databases*. NOW publishers (2011).
- [7] DE RAEDT, L., PASSERINI, A., AND TESO, S. Learning constraints from examples.
- [8] DHANABAL, L., AND SHANTHARAJAH, D. S. P. A study on nsl-kdd dataset for intrusion detection system based on classification algorithms. *International Journal of Advanced Research and Communication Engineering (IJARCCCE)* 4, 6 (2015), 446–452.
- [9] EBRAHIMI, J., RAO, A., LOWD, D., AND DOU, D. Hotflip: White-box adversarial examples for text classification. In *Proceedings of the 56th Annual Meeting of the Association for Computational Linguistics (Volume 2: Short Papers)* (2018), Association for Computational Linguistics, pp. 31–36.
- [10] FLAJOLET, P., AND MARTIN, G. N. Probabilistic counting algorithms for data base applications. *J. Comput. Syst. Sci.* 31, 2 (Sept. 1985), 182–209.
- [11] GOODFELLOW, I., PAPERNOT, N., HUANG, S., DUAN, P., ABBEEL, P., AND CLARK, J. Attacking machine learning with adversarial examples, 2017.
- [12] GOODFELLOW, I. J., SHELNS, J., AND SZEGEDY, C. Explaining and harnessing adversarial examples. *stat 1050* (2015), 20.
- [13] GROSSE, K., PAPERNOT, N., MANOHARAN, P., BACKES, M., AND MCDANIEL, P. Adversarial examples for malware detection. In *European Symposium on Research in Computer Security* (2017), Springer, pp. 62–79.
- [14] HALL, M., FRANK, E., HOLMES, G., PFAHRINGER, B., REUTEMANN, P., AND WITTEN, I. H. The WEKA data mining software: an update. *SIGKDD Explorations* 11, 1 (2009), 10–18.
- [15] HAYES, J., AND DANEZIS, G. Machine learning as an adversarial service: Learning black-box adversarial examples. *CoRR abs/1708.05207* (2017).
- [16] HUANG, G.-B., AND BABRI, H. A. Upper bounds on the number of hidden neurons in feedforward networks with arbitrary bounded nonlinear activation functions. *IEEE Transactions on Neural Networks* 9, 1 (1998), 224–229.
- [17] IBRAHIM, L. M., BASHEER, D. T., AND MAHMOUD, M. S. A comparison study for intrusion database (kdd99, nsl-kdd) based on self organization map (som) artificial neural network. *Journal of Engineering Science and Technology* 8, 1 (2013), 107–119.
- [18] ILYAS, A., ENGSTROM, L., ATHALYE, A., LIN, J., ATHALYE, A., ENGSTROM, L., ILYAS, A., AND KWOK, K. Black-box adversarial attacks with limited queries and information. In *Proceedings of the 35th International Conference on Machine Learning, {ICML} 2018* (2018).
- [19] INGRE, B., AND YADAV, A. Performance analysis of nsl-kdd dataset using ann. In *Signal Processing and Communication Engineering Systems (SPACES), 2015 International Conference on* (2015), IEEE, pp. 92–96.
- [20] JIA, R., AND LIANG, P. Adversarial examples for evaluating reading comprehension systems. In *Proceedings of the 2017 Conference on Empirical Methods in Natural Language Processing* (2017), Association for Computational Linguistics, pp. 2021–2031.
- [21] JUOLA, P., ET AL. Authorship attribution. *Foundations and Trends® in Information Retrieval* 1, 3 (2008), 233–334.
- [22] KINGMA, D. P., AND BA, J. Adam: A method for stochastic optimization. *CoRR abs/1412.6980* (2014).
- [23] KOLOSNAJI, B., DEMONTIS, A., BIGGIO, B., MAIORCA, D., GIACINTO, G., ECKERT, C., AND ROLI, F. Adversarial malware binaries: Evading deep learning for malware detection in executables. In *2018 26th European Signal Processing Conference (EUSIPCO)* (Sep. 2018), pp. 533–537.
- [24] KOUROU, K., EXARCHOS, T. P., EXARCHOS, K. P., KARAMOUZIS, M. V., AND FOTIADIS, D. I. Machine learning applications in cancer prognosis and prediction. *Computational and Structural Biotechnology Journal* 13 (2015), 8 – 17.
- [25] KURAKIN, A., GOODFELLOW, I. J., AND BENGIO, S. Adversarial examples in the physical world. In *International Conference on Learning Representations Workshop* (2017).
- [26] LECUN, Y., BOTTOU, L., BENGIO, Y., AND HAFFNER, P. Gradient-based learning applied to document recognition. *Proceedings of the IEEE* 86, 11 (Nov 1998), 2278–2324.
- [27] MADRY, A., MAKELOV, A., SCHMIDT, L., TSIPRAS, D., AND VLADU, A. Towards deep learning models resistant to adversarial attacks. In *International Conference on Learning Representations* (2018).
- [28] MOOSAVI-DEZFOOLI, S., FAWZI, A., AND FROSSARD, P. Deepfool: A simple and accurate method to fool deep neural networks. In *2016 IEEE Conference on Computer Vision and Pattern Recognition (CVPR)* (June 2016), pp. 2574–2582.
- [29] MOOSAVI-DEZFOOLI, S. M., FAWZI, A., FAWZI, O., AND FROSSARD, P. Universal adversarial perturbations. In *2017 IEEE Conference on Computer Vision and Pattern Recognition (CVPR)* (July 2017), pp. 86–94.
- [30] MOUSTAFA, N., AND SLAY, J. Unsw-nb15: a comprehensive data set for network intrusion detection systems (unsw-nb15 network data set). In *Military Communications and Information Systems Conference (MilCIS), 2015* (2015), IEEE, pp. 1–6.
- [31] MOUSTAFA, N., AND SLAY, J. The evaluation of network anomaly detection systems: Statistical analysis of the unsw-nb15 data set and the comparison with the kdd99 data set. *Information Security Journal: A Global Perspective* 25, 1-3 (2016), 18–31.
- [32] PAPERNOT, N., CARLINI, N., GOODFELLOW, I., FEINMAN, R., FAGHRI, F., MATYASKO, A., HAMBARDZUMYAN, K., JUANG, Y.-L., KURAKIN, A., SHEATSLEY, R., ET AL. Cleverhans v2. 0.0: an adversarial machine learning library. *arXiv preprint arXiv:1610.00768* (2016).
- [33] PAPERNOT, N., MCDANIEL, P., JHA, S., FREDRIKSON, M., CELIK, Z. B., AND SWAMI, A. The limitations of deep learning in adversarial settings. In *Security and Privacy (EuroS&P), 2016 IEEE European Symposium on* (2016), IEEE, pp. 372–387.
- [34] PAPERNOT, N., MCDANIEL, P. D., AND GOODFELLOW, I. J. Transferability in machine learning: from phenomena to black-box attacks using adversarial samples. *CoRR abs/1605.07277* (2016).
- [35] POMERLEAU, D. A. Efficient training of artificial neural networks for autonomous navigation. *Neural Computation* 3, 1 (1991), 88–97.
- [36] SHARIF, M., BHAGAVATULA, S., BAUER, L., AND REITER, M. K. Accessorize to a crime: Real and stealthy attacks on state-of-the-art face recognition. In *Proceedings of the 2016 ACM SIGSAC Conference on Computer and Communications Security* (2016), ACM, pp. 1528–1540.
- [37] SINCLAIR, C., PIERCE, L., AND MATZNER, S. An application of machine learning to network intrusion detection. In *Computer Security Applications Conference, 1999.(ACSAC'99) Proceedings. 15th Annual* (1999), IEEE, pp. 371–377.
- [38] SOMMER, R., AND PAXSON, V. Outside the closed world: On using machine learning for network intrusion detection. In *Security and Privacy (SP), 2010 IEEE Symposium on* (2010), IEEE, pp. 305–316.
- [39] STALKAMP, J., SCHLIPSING, M., SALMEN, J., AND IGEL, C. Man vs. computer: Benchmarking machine learning algorithms for traffic sign recognition. *Neural Networks*, 0 (2012), –.
- [40] STAŃCZYK, U., AND CYRAN, K. A. Machine learning approach to authorship attribution of literary texts. *International journal of applied mathematics and informatics* 1, 4 (2007), 151–158.
- [41] SZEGEDY, C., ZAREMBA, W., SUTSKEVER, I., BRUNA, J., ERHAN, D., GOODFELLOW, I., AND FERGUS, R. Intriguing properties of neural networks. *arXiv preprint arXiv:1312.6199* (2013).
- [42] TAVALLAE, M., BAGHERI, E., LU, W., AND GHORBANI, A. A. A detailed analysis of the kdd cup 99 data set. In *Computational Intelligence for Security and Defense Applications, 2009. CISDA 2009. IEEE Symposium on* (2009), IEEE, pp. 1–6.
- [43] TIBSHIRANI, R. Regression shrinkage and selection via the lasso. *Journal of the Royal Statistical Society. Series B (Methodological)* 58, 1 (1996), 267–288.
- [44] TRAMÈR, F., PAPERNOT, N., GOODFELLOW, I., BONEH, D., AND MCDANIEL, P. The space of transferable adversarial examples. *arXiv preprint arXiv:1704.03453* (2017).
- [45] TSAI, C.-F., HSU, Y.-F., LIN, C.-Y., AND LIN, W.-Y. Intrusion detection by machine learning: A review. *Expert Systems with Applications* 36, 10 (2009), 11994–12000.
- [46] WONG, B. K., BODNOVICH, T. A., AND SELVI, Y. Neural network applications in business: A review and analysis of the literature (1988–1995). *Decision Support Systems* 19, 4 (1997), 301–320.

8 APPENDIX

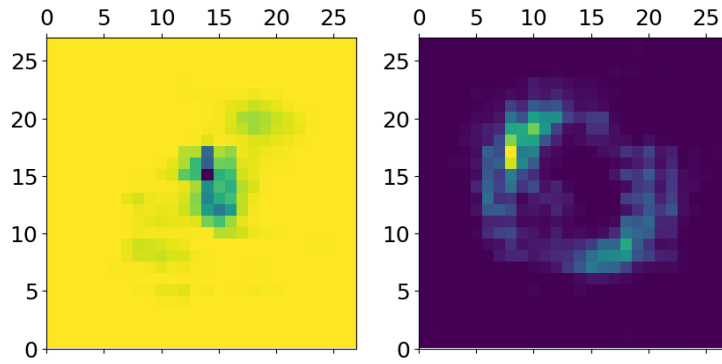
Protocol	Feature Type			
	Basic	Content	Timing-based	Host-based
TCP	duration, service=aol, service=auth, service=bgp, service=courier, service=csnet_ns, service=ctf, service=daytime, service=discard, service=domain, service=echo, service=efs, service=exec, service=finger, service=ftp, service=ftp_data, service=gopher, service=harvest, service=hostnames, service=http, service=http_2784, service=http_443, service=http_8001, service=IRC, service=iso_tsap, service=klogin, service=kshell, service=ldap, service=link, service=login, service=mtp, service=name, service=netbios_dgm, service=netbios_ns, service=netbios_ssn, service=netstat, service=nntp, service=nntp, service=other, service=pm_dump, service=pop_2, service=pop_3, service=printer, service=private, service=remote_job, service=rje, service=shell, service=sntp, service=sql_net, service=ssh, service=sunrpc, service=supdup, service=systat, service=telnet, service=time, service=uucp, service=uucp_path, service=vmnet, service=whois, service=X11, service=Z39_50, service=34, flag=OTH, flag=REJ, flag=RSTO, flag=RSTOS0, flag=RSTR, flag=S0, flag=S1, flag=S2, flag=S3, flag=SF, flag=SH, src_bytes, dst_bytes, land=1, urgent	hot, num_failed_logins, logged_in=1, num_compromised, root_shell, su_attempted, num_root, num_file_creations, num_shells, num_access_files, is_host_login=1, is_guest_login=1	count, srv_count, error_rate, srv_error_rate, error_rate, srv_error_rate, same_srv_rate, diff_srv_rate, srv_diff_host_rate	dst_host_count, dst_host_srv_count, dst_host_same_srv_rate, dst_host_diff_srv_rate, dst_host_same_src_port_rate, dst_host_srv_diff_host_rate, dst_host_error_rate, dst_host_srv_error_rate, dst_host_error_rate, dst_host_srv_error_rate
UDP	duration, service=domain_u, service=ntp_u, service=other, service=private, service=tftp_u, flag=SF, wrong_fragment		count, srv_count, error_rate, error_rate, same_srv_rate, diff_srv_rate, srv_diff_host_rate	dst_host_count, dst_host_srv_count, dst_host_same_srv_rate, dst_host_diff_srv_rate, dst_host_same_src_port_rate, dst_host_srv_diff_host_rate, dst_host_error_rate, dst_host_error_rate
ICMP	service=eco_i, service=ecr_i, service=red_i, service=tim_i, service=urh_i, service=urp_i, flag=SF, src_bytes, wrong_fragment		count, srv_count, error_rate, error_rate, same_srv_rate, diff_srv_rate, srv_diff_host_rate	dst_host_count, dst_host_srv_count, dst_host_same_srv_rate, dst_host_diff_srv_rate, dst_host_same_src_port_rate, dst_host_srv_diff_host_rate, dst_host_error_rate, dst_host_error_rate

Table 5: The constraints extracted from the NSL-KDD - Unlike TCP, UDP and ICMP have limited degrees of freedom.

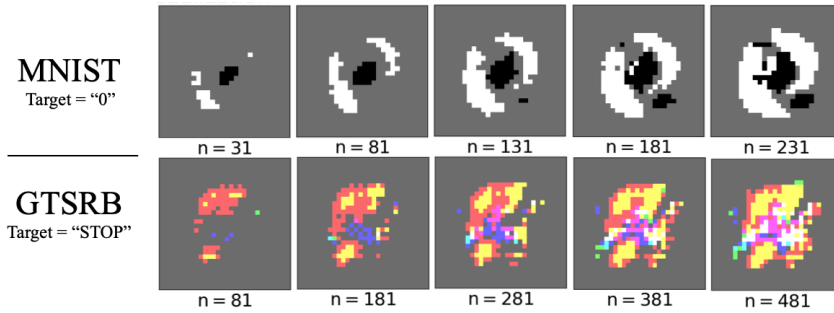
Learning Technique	Parameters		Test Accuracy			
	Name	Value	NSL-KDD	UNSW-NB15	MNIST	GTSRB
Logistic Regression	PENALTY	l2	74.21%	67.65%	92.02%	84.94%
	C	1.0				
Support Vector Machine	C	1.0	77.31%	69.02%	94.04%	84.3%
	KERNEL	rbf				
	DEGREE	3				
Decision Tree Classifier	CRITERION	gini	74.52%	73.27%	87.73%	57.20%
	MAX_DEPTH	∞				
	MIN_SAMPLES_SPLIT	2				
	MIN_SAMPLES_LEAF	1				
k-Nearest Neighbor	MAX_FEATURES	∞	74.90%	72.20%	96.88%	52.83%
	K	5				
	P	2				

Table 6: Scikit-Learn Model Information

Model M_A MNIST Negative & Positive Perturbation Heatmaps



(a) Perturbation Histogram produced by the AJSMA for the MNIST model M_A as a 2D Heatmap - The target class ("0") can be visibly seen by combining the decreasing features plot (left) with the increasing features plot (right).



(b) Sketch Visualization for MNIST and GTSRB for varying values of n - As n increases, the target class visibly forms.

Figure 6: Perturbation Histogram for MNIST (a) and adversarial sketches for image datasets (b).